The role of EXT and growth signalling pathways in osteochondroma and its progression towards secondary peripheral chondrosarcoma

Hameetman, L.

Peripheral chondrosarcoma progression is accompanied by decreased Indian Hedgehog (IHH) signalling

5

Liesbeth Hameetman, Leida B. Rozeman,
Marcel Lombaerts, Jan Oosting,
Antonie H.M. Taminiau,
Anne-Marie Cleton-Jansen,
Judith V.M.G. Bovée,
Pancras C.W. Hogendoorn

Journal of Pathology
(2006); 209(4): 501-511

Abstract
Hedgehog (HH) signalling is important for specific developmental processes, and aberrant, increased activity has been described in various tumours. Disturbed HH signalling has also been implicated in the hereditary syndrome, Multiple Osteochondromas. Indian Hedgehog (IHH), together with parathyroid hormone-like hormone (PTHLH), participates in the organization of growth plates in long bones. PTHLH signalling is absent in osteochondromas, benign tumours arising adjacent to the growth plate, but is reactivated when these tumours undergo malignant transformation towards secondary peripheral chondrosarcoma. We describe a gradual decrease in the expression of *Patched* (*PTCH*) and *glioma-associated oncogene homolog 1* (*GLI1*) (both transcribed upon IHH activity), and *GLI2* with increasing malignancy, suggesting that IHH signalling is inactive and PTHLH signalling is IHH independent in secondary peripheral chondrosarcomas. cDNA expression profiling and immunohistochemical studies suggest that transforming growth factor-β (TGF-β)-mediated proliferative signalling is active in high-grade chondrosarcomas since TGF-β downstream targets were upregulated in these tumours. This is accompanied by downregulation of energy metabolism-related genes and upregulation of the proto-oncogene *jun B*. Thus, the tight regulation of growth plate organization by IHH signalling is still seen in osteochondroma, but gradually lost during malignant transformation to secondary peripheral chondrosarcoma and subsequent progression. TGF-β signalling is stimulated during secondary peripheral chondrosarcoma progression and could potentially regulate the retained activity of PTHLH.

Keywords: Hedgehog; transforming growth factor-β; cartilaginous tumours; molecular pathways; tumour progression

Introduction

Hedgehog (HH) signalling plays an important role during embryonic and postembryonic development, where it regulates cell proliferation and/or differentiation [1]. Upon binding to HH, Patched (PTCH) relieves its inhibition of Smoothened (SMO), which activates GLI transcription factor family members (GLI1-3). This leads to activation of target genes, including GLI1 and PTCH itself [2,3]. In the growth plate, Indian Hedgehog (IHH) regulates chondrocyte proliferation and differentiation in a tightly regulated paracrine feedback loop, together with parathyroid hormone-like hormone (PTHLH or PTHrP; figure 5.1A) [4,5,7].

Deregulated IHH signalling has been implicated in patients with Multiple Osteochondromas [8-10], an autosomal dominant disorder characterized by the formation of cartilage-capped, benign, bony neoplasms on the outer surface of bones preformed by endochondral ossification [9,11]. *EXT1* and *EXT2* have been identified as tumour suppressor genes for Multiple Osteochondromas [12]. These genes are involved in the biosynthesis of heparan sulphate proteoglycans (HSPGs) [13,14], multifunctional macromolecules involved in the diffusion of HH to PTCH [10,15]. Osteochondromas also occur as solitary lesions in a non-hereditary background[11]. The cartilage cap of osteochondromas morphologically recapitulates the epiphyseal growth plate [11].

A small fraction (<3%) of osteochondromas transforms into so-called secondary peripheral chondrosarcoma [16,17], which are classified histologically into three grades that correlate with prognosis [18]. Condrosarcomas can recur at a higher histological grade [16], suggesting progression in malignancy with time.

Recent findings have linked upregulated HH signalling to various human diseases [2], such as Gorlin syndrome, in which HH signalling is constitutively active as a result of inactivating mutations in *PTCH* [19]. Moreover, constitutively active HH signalling has been found in several sporadic cancers, including sporadic basal cell carcinoma [20], medulloblastoma [21], colon cancer[22], small-cell lung cancer [23] and prostate cancer [24]. Inactivation of HH signalling has been associated with developmental malformations such as cyclopia and holoprosencephaly [2].

The involvement of IHH signalling in tumourigenesis as well as endochondral ossification points to its possible involvement in osteochondroma and chondrosarcoma. We have previously demonstrated that molecules downstream in the IHH/PTHLH signalling pathway are not expressed in osteochondromas [25,26], suggesting that growth signalling is disturbed. Malignant transformation leads to re-expression of these signalling molecules [25,26].

Here, we aimed at elucidating the role of IHH signalling in the progression of peripheral chondrosarcomas, in a series of hereditary and sporadic osteochondromas, as well as chondrosarcomas. The same series was subjected to genome-wide expression analysis to identify other signal transduction pathways involved in chondrosarcoma progression.

Material and methods

Patient material

Fresh frozen samples were obtained from resected specimens (table V.I). Growth plates were acquired from resections or biopsies for orthopaedic clinical conditions not related to osteochondroma or chondrosarcoma. All tissue samples were handled in a coded fashion, according to Dutch national ethical guidelines ("Code for Proper Secondary Use of Human Tissue", Dutch Federation of Medical Scientific Societies).

RNA isolation

RNA was isolated from tumour samples that contained at least 70% tumour cells, as determined by haematoxylin and eosin stained frozen sections, as described previously [27]. From L-493, RNA was isolated from two different parts of the tumour (one part corresponding to a low-grade area and the other with high-grade morphology), to investigate possible differences in gene expression within one tumour.

Quantitative reversed transcriptase PCR (qPCR)

For first strand cDNA synthesis, 1 μg of total RNA was reverse transcribed using AMV reverse transcriptase (Roche, Penzberg, Germany) with 100 ng primer (dT) 15 (Roche) and 50 ng random primers (Invitrogen, Carlsbad CA, USA), according to the manufacturer's instructions.

qPCR reactions were performed as previously described [28] with PCR primers provided in supplementary table V.I. Expression levels were normalized to four genes (*CPSF6*, *GPR108*, *CAPNS1,* and *SRPR*) selected from expression profiling experiments of peripheral and central[29] cartilaginous tumours, with the least variation between all samples using the geNorm programme [30]. Log_2 transformed normalized data were analysed in SPSS 11.0 (SPSS Inc., Chicago, IL, USA). Expression levels in human growth plates were compared with those in osteochondromas, low-grade (grade I) and high-grade (grade II and III) chondrosarcomas using one-way ANOVA with Bonferroni correction. Spearman's non-parametric correlation coefficients were computed for relations between expression levels and histological grade. Corrected p-values ≤ 0.05 were considered significant.

cDNA microarrays

A custom-made cDNA microarray was used in order to include more genes involved in chondrogenesis. The list of cDNA clones is available upon request. Array production, hybridization and image acquisition procedures were performed as described previously [29]. In brief, tumour and growth plate samples were hybridized against a common reference panel of cell lines [29,31]. For hybridization, 1 μg of sample total RNA and 1 μg of reference panel total RNA were used to generate biotin- and fluorescein-labelled cDNA, using the Micromax TSA labelling kit (Perkin Elmer, Wellesley, MA, USA). Hybridized slides were scanned with a GeneTac LSV scanner (Genomic Solutions, Ann Arbor, MI, USA). Experimental quality was checked by labelling and hybridizing five samples in duplicate, either as experimental duplicates (n=2) or dye swaps (n=3).

Data analysis

Signal intensities were recorded and quantified with Genepix Pro 4.1 software (Axon Instruments, Union City, CA, USA). A Microsoft Excel macro [29] was created to select bona fide spots systematically, normalize these by dividing by the median of all bona fide spots and log transform the normalized spots.

Analysis was performed for genes expressed in at least 70% of samples. Unsupervised hierarchical clustering (with "complete linkage" and "correlation") was performed with Spotfire Decisionsite™ software for functional genomics (Somerville, MA, USA). Two methods for group comparison were used. The first method (corrected *t*-test method) used the log-transformed ratios of the Excel macro. *P*-values were calculated by a two-sided Student's

Table V.I. Clinocopathological and tumour data

Sample	Material[a]	MO[b]/ solitary	Location	Gender	Age (yrs)	Included in experiments[c]
GP-29	GP	-	Knee	Female	12	Array, qPCR
GP-53	GP	-	Hip	Female	12	Array, qPCR
GP-62	GP	-	Femur	Female	8	Array, qPCR[d]
GP-67	GP	-	Unknown	Male	12	Array, qPCR
L-298	OC	MO	Pelvis	Male	24	Array, qPCR
L-524	OC	MO	Fibula	Male	27	Array
L-657	OC	Solitary	Femur	Female	12	Array, qPCR[d]
L-673	OC	Solitary	Humerus	Male	12	qPCR
L-841	OC	MO	Femur	Female	14	Array, qPCR[d]
L-1235	OC	MO	Radius	Female	5	Array, qPCR[d]
L-1247	OC	Solitary	Femur	Male	30	qPCR
L-114	PCS-I	MO	Femur	Male	39	qPCR
L-144	PCS-I	Solitary	Scapula	Male	28	Array
L-163	PCS-I	Solitary	Tibia	Male	49	Array, qPCR
L-626	PCS-I	Solitary	Femur	Male	21	Array, qPCR[d]
L-627	PCS-I	Solitary	Scapula	Female	31	Array, qPCR
L-724	PCS-I	Solitary	Ilium	Female	82	Array, qPCR
L-739	PCS-I	Solitary	Pubis	Male	37	Array, qPCR
L-758	PCS-I	MO	Femur	Male	41	Array, qPCR
L-868	PCS-I	Solitary	Humerus	Male	18	Array, qPCR
L-1190	PCS-I	MO	Humerus	Female	16	qPCR
L-1245	PCS-I	Solitary	Fibula	Male	25	Array, qPCR
L-11	PCS-II	Solitary	Ilium	Male	49	qPCR
L-76	PCS-II	Solitary	Pelvis	Male	47	Array, qPCR
L-123	PCS-II	Solitary	Femur	Male	60	Array, qPCR
L-224	PCS-II	Solitary	Ilium	Male	26	qPCR
L-308	PCS-II	MO	Scapula	Male	42	qPCR
L-493	PCS-II	Solitary	Thorax	Male	37	Array, qPCR[d]
L-1165	PCS-II	Solitary	Pelvis	Female	37	Array, qPCR
L-281	PCS-III	Solitary	Scapula	Female	39	Array, qPCR[d]
L-300	PCS-III	MO	Scapula	Female	61	Array, qPCR[d]

[a] GP = growth plate; OC = osteochondroma; PCS = peripheral secondary chondrosarcoma grade I, II or III.
[b] MO = Multiple Osteochondromas.
[c] Array = cDNA microarray; qPCR = quantitative reverse transcriptase PCR experiments.
[d] Samples used for standard curve in the qPCR experiments.

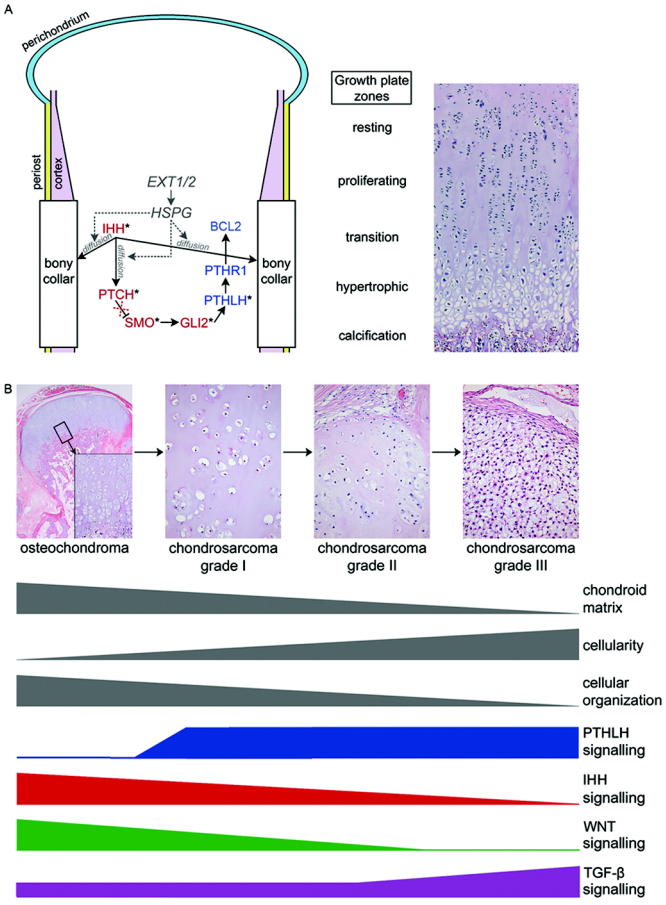

Figure 5.1. Schematic representations of signalling pathways in growth plate, osteochondromas, and chondrosarcomas. (A) IHH/PTHLH signalling in the postnatal growth plate. The IHH/PTHLH feedback loop is confined to the growth plate. In the transition zone, IHH will bind PTCH, relieving its inhibitory effect on Smoothened (SMO). SMO then activates the transcription factor GLI2, which subsequently moves to the nucleus to start transcription of IHH target genes. One of these targets is PTHLH. After PTHLH binds to its receptor PTHR1, BCL2 is upregulated, inhibiting chondrocyte differentiation (adapted from Amling et al.[4], Van der Eerden et al. [5], Mo et al. [6] and Hogendoorn et al. [7]). If EXT proteins are defective or absent, HSPG expression at the cell surface may be altered or absent, affecting the diffusion of IHH to its receptor. IHH signalling molecules are indicated in red, PTHLH signalling molecules in blue, and molecules investigated by quantitative reversed transcriptase polymerase chain reaction (qPCR) by *. (B) Schematic representation of changes in extracellular matrix, cellularity, and the expression of signalling pathways in the course of malignant transformation of osteochondromas and subsequent progression of peripheral chondrosarcoma. The different tumour types are represented by their histology. Malignant transformation of osteochondromas and further progression of peripheral chondrosarcoma are characterized by a decrease in chondroid matrix and an increase in cellularity, and the strict organization seen in growth plate is lost. In osteochondromas, there is IHH, canonical WNT and TGF-β signalling but no PTHLH signalling. During malignant transformation of tumour cells that have escaped from the tight control of IHH, PTHLH signalling is activated, but WNT signalling decreases. During the progression of grade I towards grade III lesions, IHH signalling gradually diminishes and WNT signalling is lost. The proliferative TGF-β signalling pathway is upregulated during progression and activates target genes needed to acquire a more malignant phenotype.

t-test with unequal variance and corrected for multiple testing using the step-up procedure with a false discovery rate of 10% [32]. The second method was the Limma (Linear models for Microarray Data) package [33], because of its excellent performance in microarray analysis. Limma used the raw Genepix data for within-array print-tip loess normalization of intensities after the same criteria for spot selection were applied, as described in the Excel macro [29]. Identities of differentially expressed, spotted clones were verified by sequencing the PCR products.

Differentially expressed genes were selected for verification by either qPCR or immunohistochemistry. The micro-array series could be expanded with seven extra tumours (table V.I) for qPCR analysis.

Immunohistochemistry

Expression of JUNB (antibody sc-8051, Santa Cruz Biotechnology Inc., Santa Cruz, CA, USA, dilution 1:150) and PAI1 (*SERPINE1* protein; antibody #3785, American Diagnostica, Stanford, CT, USA, dilution 1:350) was evaluated in 18 osteochondromas, 39 chondrosarcomas, and 12 human growth plates. Staining and scoring of 4-μm sections of formalin-fixed, paraffin-embedded material was performed as described [25]. Staining intensity was compared with internal positive controls: osteoblasts and osteoclasts for JUNB, blood vessels and connective tissue for PAI1.

Activity of TGF-β signalling and WNT-signalling was investigated by presence of either nuclear phosphorylated Smad2 (PS2 antibody, kindly donated by P. ten Dijke [34], dilution 1:2000) expression or nuclear β-catenin (clone 14, BD Biosciences, Erembodegem, Belgium, dilution 1:800) expression. Osteoblasts served as positive internal control for PS2, and osteoblasts and blood vessels for β-catenin.

A χ^2 test and Spearman's non-parametric correlation were used in the statistical analysis. Values of $P \leq 0.05$ were considered significant.

Results

qPCR to detect mRNA expression of IHH signalling molecules

Expression of seven genes involved in IHH signalling (figure 5.1A) was assayed using qPCR, and compared to human growth plates (table V.II). Compared with growth plates, *PTCH* expression was decreased in low-grade (p = 0.039) and high-grade chondrosarcomas (p = 0.001) but not in osteochondromas (p = 1.00; figure 5.2A). Of the *GLI* transcription factors, *GLI2* had the highest expression in the growth plate (p = 0.006) and was reduced in low-grade chondrosarcomas (p = 0.015). Expression of both *GLI2* and *GLI1* was even lower in high-grade tumours compared to growth plate (p = 0.002 and p = 0.043, respectively; figure 5.2B-C). *GLI1* expression correlated with *GLI2* expression (r = 0.584, p = 0.02). *GLI3* expression was not affected in tumours (table V.II).

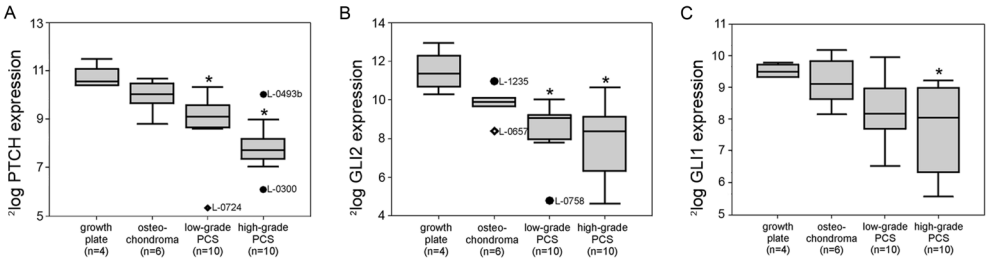

Figure 5.2. qPCR results of IHH signalling molecules.(A-C) Log-transformed relative mRNA expression levels in growth plate, osteochondromas, and low-grade and high-grade chondrosarcomas represented in boxplots of (A) *PTCH* expression, (B) *GLI2* expression, and (C) *GLI1* expression. *Significantly lower expression compared to growth plate (p < 0.05), Diamonds=extreme values; filled circles=outliers; PCS=peripheral chondrosarcoma

Increasing histological grade correlated negatively to the expression of *PTCH* (r = -0.600, p = 0.001), *GLI1* (r = -0.458, p = 0.018), and *GLI2* (r = -0.457, p = 0.019), suggesting gradual downregulation of IHH signalling during tumour progression (figure 5.1B). Expression of *PTCH* (r = -0.810, $p < 0.001$), *GLI1* (r = -0.524, p = 0.006), and *GLI2* (r = -0.421, p = 0.032) correlated negatively with patient age (supplementary figure 5.1), gradually diminishing over 40 years. Using age as a covariate in the analysis, the difference in expression between growth plates and chondrosarcomas was only significant for *GLI2* (p = 0.034).

For the grade II chondrosarcoma L-493, two separate tissue samples were used. Expression data from the matrix-rich sample were similar to those of low-grade tumours, while results from the more cellular and myxoid sample corresponded to those of high-grade chondrosarcomas.

PTHLH mRNA expression was present in all tumours. PTHLH protein expression data, as determined previously [25], was available for four osteochondromas and 14 chondrosarcomas, and correlated with the mRNA expression (r = 0.53, p = 0.01).

Table V.II. Log_2 transformed relative expression data of *IHH* signalling molecules in qPCR

	Growth plate (n = 4)	Osteochondroma (n = 6)	*Osteochon-droma vs growth plate*	Low grade PCS[a]		*Low-grade PCS vs growth plate*	High grade PCS		*High-grade PCS vs growth plate*
Genes	**Median[b] ± SD**	**Median ± SD**	***p-value[b]***	***n***	**Median ± SD**	***p-value***	***n***	**Median ± SD**	***p-value***
IHH	10.94 ± 2.44	9.08 ± 2.62	*1.000*	9	10.34 ± 2.88	*1.000*	9	7.19 ± 2.65	*0.166*
PTCH	10.74 ± 0.54	10.22 ± 0.73	*1.000*	10	9.24 ± 1.38	***0.039***	10	7.80 ± 1.11	***0.001***
SMO	10.22 ± 0.49	10.33 ± 0.36	*1.000*	10	10.50 ± 0.66	*1.000*	10	9.73 ± 1.34	*0.554*
GLI1	9.80 ± 0.23	9.43 ± 0.75	*1.000*	10	8.49 ± 1.04	*0.235*	10	8.37 ± 1.35	***0.043***
GLI2	11.10 ± 0.93	9.87 ± 0.73	*0.567*	10	9.17 ± 1.23	***0.015***	10	8.62 ± 1.59	***0.002***
GLI3	9.65 ± 0.22	8.91 ± 0.71	*1.000*	10	9.04 ± 0.70	*1.000*	10	9.16 ± 1.00	*0.475*
PTHLH	7.44 ± 0.83	6.08 ± 1.11	*0.620*	10	5.68 ± 1.08	*0.474*	10	4.95 ± 1.89	*0.206*

[a] PCS = peripheral chondrosarcoma.
[b] Median = median log transformed expression level of the group.
[c] *P*-value after Bonferroni correction.

Expression profiling

To identify signal transduction pathways that might be alternatives to IHH signalling, genome-wide cDNA microarray analysis was performed on 20 tumours and four growth plates. Hierarchical cluster analysis showed that technical duplicates and dye swaps cluster together (supplementary figure 5.2), assuring technical reproducibility and absence of dye bias as well as the microarray quality. Duplicate spotted clones showed optimal correlation as well. The samples from L-493 with different histology did not cluster together, in contrast to technical duplicates from other samples, complying with aforementioned qPCR results. Unsupervised clustering showed no distinct clusters of tumour samples, indicating that the different histological grades are characterized by more subtle changes in gene expression. Despite the good overall quality of the microarray, 20 cDNA clones of genes involved in IHH and PTHLH signalling performed suboptimal and could therefore not be optimally correlated to the qPCR results of these genes.

Limma analysis revealed 17 differentially expressed cDNA clones between osteochondromas and human growth plates (supplementary table V.II). Fourteen clones were more highly expressed in osteochondromas, including multiple clones encoding the proto-oncogene jun B (*JUNB*) and several metallothionein 1 (*MT1*) genes.

We did not find any significantly differentially expressed genes in the comparison of osteochondroma and grade I chondrosarcoma.

A comparison of grade I and grade III chondrosarcomas for analysis of tumour progression identified 79 differentially expressed genes with the corrected *t*-test method and 32 with the Limma package (supplementary table V.III). Eleven genes were present in both analyses. Several genes involved in TGF-β signalling were upregulated in grade III chondrosarcomas: fibronectin 1(*FN1*); serine (or cysteine) proteinase inhibitor, clade E (nexin, plasminogen activator inhibitor type 1), member 1 (*SERPINE1*); thrombospondin 1 (*THBS1*); and cyclin-dependent kinase inhibitor 1A (*CDKN1A*, *p21*, *CIP1*). TGF-β1 was upregulated in high-grade chondrosarcomas (supplementary table V.III). Several genes involved in extracellular matrix (ECM) remodelling were upregulated; among the downregulated genes (corrected *t*-test n=23; Limma n=5) were those encoding the α1 chains of type IX collagen (*COL9A1*) and type II collagen (*COL2A1*). Additionally, several genes encoding proteins involved in oxidative phosphorylation were downregulated in grade III chondrosarcomas. These included genes encoding NADH dehydrogenase (ubiquinone) 1 β subcomplex, 8 (*NDUFB8*), a component of complex I, and cytochrome c oxidase subunit 8A (*COX8A*) of complex IV. Also, glycolytic enzyme aldolase C (*ALDOC*), part of the glycolysis, was downregulated in grade III chondrosarcomas compared with grade I lesions.

qPCR verification of cDNA microarray results

To confirm the differences in mRNA expression of genes relevant to TGF-β signalling, extracellular matrix and oxidative phosphorylation found in the progression analysis, we performed qPCR on four genes representing these groups (table V.III). The qPCR results for *FN1*, *PLOD3* and *NDUFB8* correlated with the microarray expression data (p = 0.006, p = 0.004 and p = 0.052 respectively). No correlation was found for *COX8A* (p = 0.948). *FN1* was upregulated in grade III chondrosarcomas compared with osteochondromas, grade I

Table V.III. Log_2 transformed normalized expression levels for verification microarray data

	Growth plate (n = 4)	Osteochondroma (n = 6)	PCS-I[a] (n = 10)	PCS-II (n = 8)	PCS-III (n = 2)	Correlation with microarray expression data[b]	
Genes	Median[c] ± SD	Median ± SD	Median ± SD	Median ± SD	Median ± SD	r	p-value
ALDOA	7.50 ± 0.41	7.61 ± 0.51	8.47 ± 0.74	8.47 ± 0.25	7.89 ± 0.02	0.509	0.013
COX8	8.39 ± 0.54	7.89 ± 0.61	8.55 ± 0.58	8.26 ± 0.67	8.19 ± 0.27	0.014	0.948
NDUFB8	11.73 ± 0.32	11.63 ± 0.71	11.98 ± 1.71	10.36 ± 0.81	10.39 ± 0.33	0.409	0.052
NDUFS3	8.50 ± 0.94	8.53 ± 0.79	8.36 ± 1.09	6.98 ± 0.69	7.13 ± 0.82	0.195	0.372
PLOD3	4.87 ± 0.44	5.18 ± 0.92	6.07 ± 0.74	6.42 ± 0.53	6.66 ± 0.38	0.579	0.004
FN1	11.36 ± 0.84	10.73 ± 1.13	10.61 ± 1.10	11.06 ± 1.29	13.50 ± 0.31	0.552	0.006

[a] PCS = peripheral chondrosarcoma
[b] Correlation of qPCR expression data with microarray expression data available for four growth plates, four osteochondromas, eight grade I, five grade II and two grade III chondrosarcomas
[c] Median = median log transformed expression level of the group

and II chondrosarcomas (p = 0.011, 0.014, and 0.012, respectively). Procollagen-lysine, 2-oxoglutarate 5-dioxygenase 3 (*PLOD3*) expression was significantly positively correlated with increasing histological grade (r = 0.506, p = 0.008), while *NDUFB8* showed a negative correlation (r= -0.391, p = 0.049). Additionally, mRNA expression of NADH dehydrogenase (ubiquinone) Fe-S protein 3 (*NDUFS3*) of oxidative phosphorylation complex I, and aldolase A (*ALDOA*) of glycolysis were analyzed. Similar to *NDUFB8*, *NDUFS3* expression was negatively correlated with tumour progression (r = -0.529, p = 0.005). Expression of *COX8* and *ALDOA* decreased with progression. *ALDOA* was upregulated in grade I chondrosarcomas when compared with osteochondromas (p = 0.024).

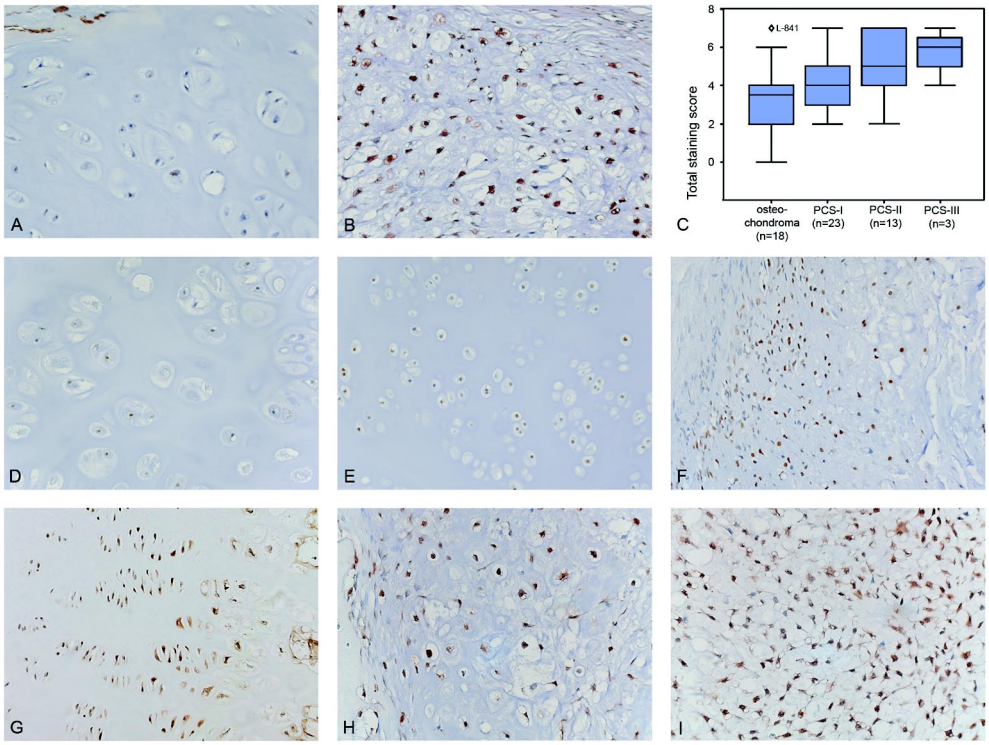

Figure 5.3. Immunohistochemical results. (A) Low-power view of an osteochondroma with weak PAI1 protein staining in less than 25% of the cells. Note the positive blood vessels, used as internal positive control; (B) a grade II chondrosarcoma with strong cytoplasmic PAI1 protein staining in 75-100% of the cells; (C) Boxplot of total scores from the semiquantitative scoring of PAI1 protein expression. There is a significant positive correlation between progression and PAI1 protein expression (r = 0.447, p < 0.001). (D) Low-power view of an osteochondroma demonstrating weak nuclear JUNB protein expression in 25-50% of the cells; (E) grade I chondrosarcoma with moderate nuclear JUNB protein expression in 75-100% of the cells; (F) Strong nuclear JUNB expression was found in most cells in this grade II chondrosarcoma. (G) Low-power view of a human epiphyseal growth plate with strong nuclear and cytoplasmic phosphorylated Smad2 staining in the proliferating and hypertrophic chondrocytes, whereas the resting chondrocytes are negative; (H) Peripheral chondrosarcoma grade II with strong phosphorylated Smad2 expression in the majority of tumour cells. The same was observed in grade III chondrosarcomas (I).

Table V.IV. Immunohistochemistry results of PAI1 and JUNB

	PAI1				JUNB[b]			
	Positive[a]		Percentage		Positive[a]		Percentage	
Growth plate					1/10	(0/2)	10	(0)
Osteochondroma	9/18	(2/3)	50	(67)	5/13	(1/3)	39	(33)
PCS grade I	15/23	(5/8)	65	(63)	7/15	(3/5)	32	(60)
PCS grade II	12/13	(4/4)	92	(100)	7/12	(2/4)	58	(50)
PCS grade III	3/3	(2/2)	100	(100)	3/3	(2/2)	100	(100)

[a] Number of positive tumours/total number of tumours that could be evaluated. Data for the tumours for which cDNA array analysis was also available are shown in parentheses.
[b] Five osteochondromas and nine chondrosarcomas could not evaluated because the internal positive controls were negative.

Immunohistochemical analysis of protein expression

SERPINE1 and *JUNB* microarray expression data were verified by immunohistochemistry (table V.IV).

The sum score of PAI1 (*SERPINE1* protein) correlated with the mRNA expression (r= 0.488, p = 0.047) and with increasing histological grade (r = 0.447, $p < 0.001$, figure 5.3A-C).

For 16 samples (two human growth plates, three osteochondromas, and five grade I, four grade II, and two grade III chondrosarcomas), also included in the microarray experiments, JUNB protein expression correlated with the mRNA expression (r = 0.544, p = 0.016). Expression analysis revealed differential expression of JUNB mRNA between growth plate and osteochondroma. When comparing growth plates and osteochondromas for JUNB protein expression, no difference was observed (Fisher's Exact, p = 0.179). The number of JUNB-positive tumours significantly correlated with increasing histological grade (χ^2 , linear-by-linear, p = 0.005, figure 5.3D-F, table V.IV).

In human growth plates, both cytoplasmic and nuclear expression of phosphorylated Smad2 was observed in proliferating and hypertrophic chondrocytes (figure 5.3G). Expression was variable in resting chondrocytes. Nuclear and cytoplasmic expression of phosphorylated Smad2 was observed in all osteochondromas and chondrosarcomas (figure 5.3H-I), implicating active TGF-β signalling (figure 5.1B).

Nuclear expression of β-catenin, was found, 9/17 (53%) osteochondromas, 4/21 (19%) grade I chondrosarcomas, and in the hypertrophic zone of 5/12 (42%) human growth plates, but not in 11 grade II and two grade III chondrosarcomas. This indicated that canonical WNT signalling decreased with increasing malignancy (χ^2 p = 0.020; figure 5.1B). Twenty-two tumours also included in the frozen series demonstrated a positive correlation between PTCH expression and nuclear expression of β-catenin (r = 0.567, p = 0.006).

Discussion

This study shows that mRNA expression of IHH downstream targets is gradually downregulated during tumour progression in peripheral chondrosarcoma compared with normal growth plates, from which its benign precursor, osteochondroma, originates. Expression of both *PTCH* and *GLI1*, two genes transcribed upon activation of HH signalling [3], negatively correlated

with increasing histological grade. This was also found for *GLI2*, which transduces the IHH signal during endochondral bone development [6], but is not a known downstream target of IHH. Recently, GLI3 has been identified as a key effector of IHH signalling during cartilage development [35], where IHH antagonises the repressor activity of GLI3 on PTHLH expression and proliferation. However, in chondrosarcomas *GLI3* expression was similar to the expression seen in human growth plate (table V.II). Therefore, there was no indication that GLI3 plays a role in chondrosarcoma progression.

Recently, constitutively active IHH signalling was demonstrated in chondrosarcoma explants [36]. These contradictory results could be partly explained by the selection of housekeeping genes for qPCR analysis. This has been shown to be tissue type specific [30], which led us to choose genes based upon the expression array results, instead of choosing random, non-tumour-specific genes, like *GAPDH*, which was not stably expressed in cartilaginous tumours. Also, no discrimination was made by Tiet et al. between peripheral and central-type chondrosarcomas [36], even though it was previously shown that these subtypes clearly have a different genetic make-up [37,38] and other distinct pathways might be operative.

IHH signalling has been shown to be upstream of canonical WNT signalling cascades required for osteogenic differentiation [39]. WNT signalling appears to be involved in chondrogenic differentiation, since we could demonstrate decreased nuclear expression of β-catenin during chondrosarcoma progression (figure 5.1B). This intriguing potential relation between IHH and WNT signalling in chondrogenesis needs further studies.

EXT1 and *EXT2* are of importance for the diffusion of IHH to its receptor [10,15,40]. Consequently, there is a strong indication that IHH signalling is important in osteochondroma formation. Here we have demonstrated that the expression of IHH signalling in osteochondromas did not differ from the expression found in growth plates. Morphologically, osteochondromas strongly resemble the epiphyseal growth plate [11], and different zones of endochondral ossification can sometimes be distinguished. It was technically not possible to dissect these different layers to investigate zone-specific expression of IHH signalling molecules. This probably also affects expression levels of genes that are only expressed in a specific layer.

Similar to growth plates, osteochondromas cease to grow after puberty [11]. Therefore we investigated the putative relationship between mRNA levels of IHH signalling molecules in tumours and patient age, and demonstrated decreasing expression of *PTCH*, *GLI1*, and *GLI2* over a period of 40 years. However, the observation that diagnosis is correlated with age [41] and the distinct expression profiles of low-grade and high-grade tumours of patients with the same age (including the two samples from L-493), suggest that expression of *PTCH*, *GLI1*, and *GLI2* does correlate with tumour progression.

Despite inactivation of IHH signalling, there is active, IHH-independent PTHLH signalling in chondrosarcomas (figure 5.1B) [4,25]. This is similar to what was found in central chondrosarcomas [28], but not to murine growth plate, where IHH has been shown to directly regulate PTHLH expression [42]. Our results showed a discrepancy between PTHLH mRNA and previously published protein expression [25]. However *PTHLH* mRNA has a very short half-life[43], making it difficult to correlate protein and gene expression.

A good candidate to activate PTHLH signalling in the absence of IHH is TGF-β, which can regulate *PTHLH* expression independent of IHH [44]. Genome-wide expression profiling

experiments revealed that tumour progression was indeed associated with upregulation of genes involved in TGF-β signalling, including TGF-β1, comparable to results found in other tumours [45]. Expression of *FN1*, *SERPINE1*, and *THBS1* was upregulated in grade III chondrosarcomas (tables V.III and V.IV). These genes are known downstream targets of TGF-β signalling and significant in regard to tumour invasion and metastasis [46]. Upregulation of the TGF-β downstream cell cycle inhibitor CDKN1A has previously been noted at the protein level [25]. The changes observed in extracellular matrix-related genes could also be regulated by TGF-β. Taken together, these results implied that TGF-β signalling is activated in high-grade chondrosarcomas and this conclusion was supported by the presence of nuclear phosphorylated Smad2 in these tumours. Phosphorylated Smad2 was also present in osteochondromas and human growth plates. For the latter the expression pattern was similar to that of unphosphorylated Smad2 in rat epiphyseal growth plate [47]. One can hypothesize that in chondrosarcomas TGF-β activates specific target genes needed to acquire a malignant phenotype. The possibility cannot be excluded that some of these differentially expressed genes, like *THBS1* and *FN1*, are the result of the increased vascularization in high-grade chondrosarcomas [48,49].

The diminished amounts of chondroid matrix in high-grade chondrosarcomas [16] and its lack of cellular organization in comparison with osteochondroma suggest loss of the IHH/PTHLH feedback loop (figure 5.1). IHH signalling is a tightly controlled signalling pathway. We observed that osteochondroma cells are still controlled by IHH and undergo endochondral ossification. As the osteochondroma ages, IHH signalling decreases, which was also seen in the growth plate [50], and all tumour cells will eventually differentiate. One can hypothesize that tumour cells may escape from IHH control to transform into a malignancy, by switching to less controlled proliferative signalling pathways, such as TGF-β signalling, thereby causing a cascade of events resulting in tumour progression (figure 5.1B). To further explore this hypothesis, a model system would be helpful, but this is hampered by differences between human and rodents, in which there is no closure of the growth plate at the end of sexual maturation [51].

Further analysis of the genome-wide expression studies revealed decreased expression of genes that encode proteins involved in oxidative phosphorylation and glycolysis in grade III chondrosarcomas compared to grade I chondrosarcomas. Glycolysis is upregulated in hypoxic environments, such as paucivascular osteochondromas and low-grade chondrosarcomas [11,16], giving cells a growth advantage [52]. High-grade chondrosarcomas show increased vascularisation [48,49], which will raise oxygen availability and thereby abolish the need for glycolysis. This was reflected by the downregulation of *ALDOA* and *ALDOC* in grade III chondrosarcomas.

Oxidative phosphorylation was simultaneously downregulated with glycolysis. In otherwise non-invasive C2C12 myoblasts, depletion of mitochondrial DNA induces an invasive phenotype [53] and increases resistance to apoptosis, in part by up-regulating BCL2 [54]. High-grade chondrosarcomas have high BCL2 expression [25] and an increased risk of recurrence and metastasis [16], consistent with an invasive phenotype.

The expression profiles of osteochondromas and grade I chondrosarcomas were indistinguishable. This distinction is also considered difficult at the histological level and is usually based on a combination of histological, radiological, and clinicopathological data [16].

Most likely the differences in gene expression are very subtle or only detectable at the protein level and cannot be detected with the method used.

Both qPCR and genome-wide expression profiling revealed similarities in gene expression between osteochondromas and human epiphyseal growth plates. However, *JUNB* (and to lesser extent *FOSB*) were more highly expressed in osteochondromas than in growth plates. JUNB and FOSB are members of the AP-1 transcription factor family, which has been implicated in endochondral ossification in mice [55,56]. Remarkably, we found very low levels of JUNB mRNA and protein in growth plates. JUNB can have a stimulatory effect on chondrocyte proliferation [55]. At the protein level, JUNB gradually increased during malignant transformation and further progression, which is consistent with its effect on proliferation. This increase in JUNB expression might also be regulated by TGF-β [57].

In conclusion, IHH signalling controls the tight regulation of growth plate organization and is still active in osteochondroma. However, IHH signalling is gradually inactivated during peripheral chondrosarcoma progression when tumour cells adapt to a more malignant phenotype (figure 5.1B). TGF-β signalling can potentially regulate PTHLH signalling and concurrent remodelling of the extracellular matrix. Downregulation of genes involved in oxidative phosphorylation and glycolysis accompanies the more invasive phenotype of high-grade tumours.

Acknowledgements

We thank P ten Dijke for providing the PS2 antibody, A Yavas, PM Wijers-Koster, HJ Baelde, and HJ van Paassen for technical assistance; P Eilers for his help with statistical analysis; R van Eijk and T van Wezel for their assistance with the cDNA array experiments; and S Romeo for fruitful discussions. This study was financially supported by the Dutch Cancer Society (grand number: RUL 2002-2738), and presented at the 18th Annual Meeting of the European MusculoSkeletal Oncology Society (EMSOS), where it was awarded the EMSOS prize. The department of Pathology, LUMC is partner of the EuroBoNeT consortium, a European Commission granted Network of Excellence for studying the pathology and genetics of bone tumours.

References

1. Nybakken K, Perrimon N. (2002) Hedgehog signal transduction: recent findings. *Curr Opin Genet Dev* **12**:503-511
2. Mullor JL, Sanchez P, Altaba AR. (2002) Pathways and consequences: Hedgehog signaling in human disease. *Trends Cell Biol* **12**:562-569
3. Ingham PW. (1998) Transducing hedgehog: the story so far. *EMBO J* **17**:3505-3511
4. Amling M, Neff L, Tanaka S, Inoue D, Kuida K, Weir E, Philbrick WM, Broadus AE, Baron R. (1997) Bcl-2 lies downstream of parathyroid hormone related peptide in a signalling pathway that regulates chondrocyte maturation during skeletal development. *J Cell Biol* **136**:205-213
5. Van der Eerden BCJ, Karperien M, Gevers EF, Lowik CWGM, Wit JM. (2000) Expression of Indian Hedgehog, PTHrP and their receptors in the postnatal growth plate of the rat: evidence for a locally acting growth restraining feedback loop after birth. *J Bone Miner Res* **15**:1045-1055
6. Mo R, Freer AM, Zinyk DL, Crackower MA, Michaud J, Heng HH, Chik KW, Shi XM, Tsui LC, Cheng SH, *et al*. (1997) Specific and redundant functions of Gli2 and Gli3 zinc finger genes in skeletal patterning and development. *Development* **124**:113-123

7. Hogendoorn PCW, Bovée JVMG, Karperien M, Cleton-Jansen AM. (2003) Skeletogenesis: Genetics. In *Nature Encyclopedia of the Human Genome*, Cooper DN (ed). Nature Publishing Group: London. pp. 306-313
8. Duncan G, McCormick C, Tufaro F. (2001) The link between heparan sulfate and hereditary bone disease: finding a function for the EXT family of putative tumor suppressor proteins. *J Clin Invest* **108**:511-516
9. Bovée JVMG, Hogendoorn PCW. (2002) Multiple osteochondromas. In *World Health Organization classification of tumours. Pathology and genetics of tumours of soft tissue and bone*, Fletcher CDM, Unni KK, Mertens F (eds). IARC Press: Lyon. pp. 360-362
10. Koziel L, Kunath M, Kelly OG, Vortkamp A. (2004) Ext1-dependent heparan sulfate regulates the range of Ihh signaling during endochondral ossification. *Dev Cell* **6**:801-813
11. Khurana J, Abdul-Karim F, Bovée JVMG. (2002) Osteochondroma. In *World Health Organization classification of tumours. Pathology and genetics of tumours of soft tissue and bone*, Fletcher CDM, Unni KK, Mertens F (eds). IARC Press: Lyon. pp. 234-236
12. Bovée JVMG, Cleton-Jansen AM, Wuyts W, Caethoven G, Taminiau AHM, Bakker E, Van Hul W, Cornelisse CJ, Hogendoorn PCW. (1999) EXT-mutation analysis and loss of heterozygosity in sporadic and hereditary osteochondromas and secondary chondrosarcomas. *Am J Hum Genet* **65**:689-698
13. McCormick C, Duncan G, Goutsos KT, Tufaro F. (2000) The putative tumor suppressors EXT1 and EXT2 form a stable complex that accumulates in the golgi apparatus and catalyzes the synthesis of heparan sulfate. *Proc Natl Acad Sci USA* **97**:668-673
14. Simmons AD, Musy MM, Lopes CS, Hwang L-Y, Yang Y-P, Lovett M. (1999) A direct interaction between EXT proteins and glycosyltransferases is defective in hereditary multiple exostoses. *Hum Mol Genet* **8**:2155-2164
15. The I, Bellaiche Y, Perrimon N. (1999) Hedgehog movement is regulated through tout velu -dependant synthesis of a heparan sulfate proteoglycan. *Mol Cell* **4**:633-639
16. Bertoni F, Bacchini P, Hogendoorn PCW. (2002) Chondrosarcoma. In *World Health Organisation classification of tumours. Pathology and genetics of tumours of soft tissue and bone*, Fletcher CDM, Unni KK, Mertens F (eds). IARC Press: Lyon. pp. 247-251
17. Bovée JVMG, Cleton-Jansen AM, Taminiau AHM, Hogendoorn PCW. (2005) Emerging pathways in the development of chondrosarcoma of bone and the implications for targeted treatment. *Lancet Oncol* **6**:599-607
18. Evans HL, Ayala AG, Romsdahl MM. (1977) Prognostic factors in chondrosarcoma of bone. A clinicopathologic analysis with emphasis on histologic grading. *Cancer* **40**:818-831
19. Hahn H, Wicking C, Zaphiropoulous PG, Gailani MR, Shanley S, Chidambaram A, Vorechovsky I, Holmberg E, Unden AB, Gillies S, *et al*. (1996) Mutations of the human homolog of Drosophila patched in the nevoid basal cell carcinoma syndrome. *Cell* **85**:841-851
20. Wolter M, Reifenberger J, Sommer C, Ruzicka T, Reifenberger G. (1997) Mutations in the human homologue of the Drosophila segment polarity gene patched (PTCH) in sporadic basal cell carcinomas of the skin and primitive neuroectodermal tumors of the central nervous system. *Cancer Res* **57**:2581-2585
21. Reifenberger J, Wolter M, Weber RG, Megahed M, Ruzicka T, Lichter P, Reifenberger G. (1998) Missense mutations in SMOH in sporadic basal cell carcinomas of the skin and primitive neuroectodermal tumors of the central nervous system. *Cancer Res* **58**:1798-1803
22. Oniscu A, James RM, Morris RG, Bader S, Malcomson RD, Harrison DJ. (2004) Expression of Sonic hedgehog pathway genes is altered in colonic neoplasia. *J Pathol* **203**:909-917
23. Watkins DN, Berman DM, Burkholder SG, Wang B, Beachy PA, Baylin SB. (2003) Hedgehog signalling within airway epithelial progenitors and in small-cell lung cancer. *Nature* **422**:313-317

24. Karhadkar SS, Steven BG, Abdallah N, Dhara S, Gardner D, Maitra A, Isaacs JT, Berman DM, Beachy PA. (2004) Hedgehog signalling in prostate regeneration, neoplasia and metastasis. *Nature* **431**:707-712
25. Bovée JVMG, Van den Broek LJCM, Cleton-Jansen AM, Hogendoorn PCW. (2000) Up-regulation of PTHrP and Bcl-2 expression characterizes the progression of osteochondroma towards peripheral chondrosarcoma and is a late event in central chondrosarcoma. *Lab Invest* **80**:1925-1933
26. Hameetman L, Kok P, Eilers PHC, Cleton-Jansen AM, Hogendoorn PCW, Bovée JVMG. (2005) The use of Bcl-2 and PTHLH immunohistochemistry in the diagnosis of peripheral chondrosarcoma in a clinicopathological setting. *Virchows Arch* **446**:430-437
27. Baelde HJ, Cleton-Jansen AM, van Beerendonk H, Namba M, Bovée JVMG, Hogendoorn PCW. (2001) High quality RNA isolation from tumours with low cellularity and high extracellular matrix component for cDNA microarrays: application to chondrosarcoma. *J Clin Pathol* **54**:778-782
28. Rozeman LB, Hameetman L, Cleton-Jansen AM, Taminiau AHM, Hogendoorn PCW, Bovée JVMG. (2005) Absence of IHH and retention of PTHrP signalling in enchondromas and central chondrosarcomas. *J Pathol* **205**:476-482
29. Rozeman LB, Hameetman L, van Wezel T, Taminiau AHM, Cleton-Jansen AM, Hogendoorn PCW, Bovée JVMG. (2005) cDNA expression profiling of central chondrosarcomas: Ollier disease resembles solitary tumors and alteration in genes coding for energy metabolism with increasing grade. *J Pathol* **207**:61-71
30. Vandesompele J, De Preter K, Pattyn F, Poppe B, Van Roy N, De Paepe A, Speleman F. (2002) Accurate normalization of real-time quantitative RT-PCR data by geometric averaging of multiple internal control genes. *Genome Biol* **3**:research0034.1-0034.11
31. Scherf U, Ross DT, Waltham M, Smith LH, Lee JK, Tanabe L, Kohn KW, Reinhold WC, Myers TG, Andrews DT, *et al*. (2000) A gene expression database for the molecular pharmacology of cancer. *Nat Genet* **24**:236-244
32. Benjamini Y, Hochberg Y. (1995) Controlling the False Discovery Rate: A Practical and Powerful Approach to Multiple Testing. *J Roy Stat Soc, Ser B* **289**:289-300
33. Smyth GK, Yang YH, Speed T. (2003) Statistical issues in cDNA microarray data analysis. *Methods Mol Biol* **224**:111-136
34. Persson U, Izumi H, Souchelnytskyi S, Itoh S, Grimsby S, Engstrom U, Heldin CH, Funa K, ten Dijke P. (1998) The L45 loop in type I receptors for TGF-beta family members is a critical determinant in specifying Smad isoform activation. *FEBS Lett* **434**:83-87
35. Hilton MJ, Tu X, Cook J, Hu H, Long F. (2005) Ihh controls cartilage development by antagonizing Gli3, but requires additional effectors to regulate osteoblast and vascular development. *Development* **132**:4339-4351
36. Tiet TD, Hopyan S, Nadesan P, Gokgoz N, Poon R, Lin AC, Yan T, Andrulis IL, Alman BA, Wunder JS. (2006) Constitutive hedgehog signaling in chondrosarcoma up-regulates tumor cell proliferation. *Am J Pathol* **168**:321-330
37. Bovée JVMG, Cleton-Jansen AM, Kuipers-Dijkshoorn N, Van den Broek LJCM, Taminiau AHM, Cornelisse CJ, Hogendoorn PCW. (1999) Loss of heterozygosity and DNA ploidy point to a diverging genetic mechanism in the origin of peripheral and central chondrosarcoma. *Genes Chrom Cancer* **26**:237-246
38. Bovée JVMG, Royen Mv, Bardoel AFJ, Rosenberg C, Cornelisse CJ, Cleton-Jansen AM, Hogendoorn PCW. (2000) Near-haploidy and subsequent polyploidization characterize the progression of peripheral chondrosarcoma. *Am J Pathol* **157**:1587-1595
39. Hu H, Hilton MJ, Tu X, Yu K, Ornitz DM, Long F. (2005) Sequential roles of Hedgehog and Wnt signaling in osteoblast development. *Development* **132**:49-60

40. Bornemann DJ, Duncan JE, Staatz W, Selleck S, Warrior R. (2004) Abrogation of heparan sulfate synthesis in Drosophila disrupts the Wingless, Hedgehog and Decapentaplegic signaling pathways. *Development* **131**:1927-1938
41. Mulder JD, Schütte HE, Kroon HM, Taconis WK. (1993) *Radiologic atlas of bone tumors* (2 edn). Elsevier: Amsterdam
42. Vortkamp A, Lee K, Lanske B, Segre GV, Kronenberg HM, Tabin CJ. (1996) Regulation of rate of cartilage differentiation by indian hedgehog and PTH-related protein. *Science* **273**:613-622
43. Sellers RS, Capen CC, Rosol TJ. (2002) Messenger RNA stability of parathyroid hormone-related protein regulated by transforming growth factor-beta1. *Mol Cell Endocrinol* **188**:37-46
44. Ferguson CM, Schwarz EM, Puzas JE, Zuscik MJ, Drissi H, O'Keefe RJ. (2004) Transforming growth factor-beta1 induced alteration of skeletal morphogenesis in vivo. *J Orthop Res* **22**:687-696
45. Blobe GC, Schiemann WP, Lodish HF. (2000) Role of transforming growth factor beta in human disease. *N Engl J Med* **342**:1350-1358
46. Berking C, Takemoto R, Schaider H, Showe L, Satyamoorthy K, Robbins P, Herlyn M. (2001) Transforming growth factor-beta1 increases survival of human melanoma through stroma remodeling. *Cancer Res* **61**:8306-8316
47. Sakou T, Onishi T, Yamamoto T, Nagamine T, Sampath T, ten Dijke P. (1999) Localization of Smads, the TGF-beta family intracellular signaling components during endochondral ossification. *J Bone Miner Res* **14**:1145-1152
48. Geirnaerdt MJ, Bloem JL, Eulderink F, Hogendoorn PCW, Taminiau AHM. (1993) Cartilaginous tumors: correlation of gadolinium-enhanced MR imaging and histopathologic findings. *Radiology* **186**:813-817
49. Ayala G, Liu C, Nicosia R, Horowitz S, Lackman R. (2000) Microvasculature and VEGF expression in cartilaginous tumors. *Hum Pathol* **31**:341-346
50. Kindblom JM, Nilsson O, Hurme T, Ohlsson C, Savendahl L. (2002) Expression and localization of Indian hedgehog (Ihh) and parathyroid hormone related protein (PTHrP) in the human growth plate during pubertal development. *J Endocrinol* **174**:R1-R6
51. Hughes PC, Tanner JM. (1970) The assessment of skeletal maturity in the growing rat. *J Anat* **106**:371-402
52. Gatenby RA, Gillies RJ. (2004) Why do cancers have high aerobic glycolysis? *Nat Rev Cancer* **4**:891-899
53. Amuthan G, Biswas G, Zhang SY, Klein-Szanto A, Vijayasarathy C, Avadhani NG. (2001) Mitochondria-to-nucleus stress signaling induces phenotypic changes, tumor progression and cell invasion. *EMBO J* **20**:1910-1920
54. Biswas G, Anandatheerthavarada HK, Avadhani NG. (2005) Mechanism of mitochondrial stress-induced resistance to apoptosis in mitochondrial DNA-depleted C2C12 myocytes. *Cell Death Differ* **12**:266-278
55. Eferl R, Wagner EF. (2003) AP-1: a double-edged sword in tumorigenesis. *Nat Rev Cancer* **3**:859-868
56. Hess J, Hartenstein B, Teurich S, Schmidt D, Schorpp-Kistner M, Angel P. (2003) Defective endochondral ossification in mice with strongly compromised expression of JunB. *J Cell Sci* **116**:4587-4596
57. Laiho M, Ronnstrand L, Heino J, Decaprio JA, Ludlow JW, Livingston DM, Massague J. (1991) Control of junB and extracellular matrix protein expression by transforming growth factor-beta 1 is independent of simian virus 40 T antigen-sensitive growth-sensitive growth-inhibitory events. *Mol Cell Biol* **11**:972-978

Supplementary material

Supplementary table V.I. Genes investigated by quantitative PCR analysis

Gene symbol	Gene name	Reference sequence	Forward primer[a]	Reverse primer
IHH	Indian hedgehog homolog (Drosophila)	NM_002181	CCAATTACAATCCAGACATCATCTTC	GATAGCCAGCGAGTTCAGGC
PTCH	patched homolog (Drosophila)	NM_000264	CCACGACAAAGCCGACTACAT	GCTGCAGATGGTCCTTACTTTTTC
SMO	smoothened homolog (Drosophila)	NM_005631	AGCGCAGCTTCCGGG	CAGTTCCAAACATGGCAAACAG
GLI1	glioma-associated oncogene homolog	NM_005269	TGCAGTAAAGCCTTCAGCAATG	TTTTCGCAGCGAGCTAGGAT
GLI2	GLI-Kruppel family member GLI2	NM_005270	TTCTCCAACGCCTCGGAC	GTGGACCGTTTTCACATGCTT
GLI3	GLI-Kruppel family member GLI3	NM_000168	TTCTCAAATGCCTCTGATCGC	CCTGGGATTTTGCACACATATG
PTHLH	parathyroid hormone-like hormone	NM_002820	CGGTGTTCCTGCTGAGCTAC	ATCGTCGCCGTAAATCTTGGAT
COX8	cytochrome c oxidase subunit 8A	NM_004074	CGCGCCAAGATCCATTCGTT	GAAGGTCACGAAGCAGGAGGT
NDUFB8	NADH dehydrogenase (ubiquinone) 1 beta subcomplex, 8	NM_005004	CGGTTTCCTGGCTTTCATGATATT	TAGTGAACCACCCGCTCTGG
NDUFS3	NADH dehydrogenase (ubiquinone) Fe-S protein 3	NM_004551	GGCTTCGAGGGACATCCTTTC	CGGAACTCTTGGGCCAACTC
PLOD3	procollagen-lysine, 2-oxoglutarate 5-dioxygenase 3	NM_001084	CCCGAGTGTGAGTTCTACTTCAG	GGGCGATCACCTTCCTGTTC
FN1	Fibronectin 1	NM_002026	GGAGAATTCAAGTGTGACCCTCA	TGCCACTGTTCTCCTACGTGG
Normalisation genes				
CPSF6	cleavage and polyadenylation specific factor 6	NM_007007	AAGATTGCCTTCATGGAATTGAG	TCGTGATCTACTATGGTCCCTCTCT
SRPR	signal recognition particle receptor	NM_003139	CATTGCTTTTGCACGTAACCAA	ATTGTCTTGCATGCGGCC
GPR108	G protein-coupled receptor 108	XM_290854	AGATGCCCCTTTTCAAGCTCTAC	GCCATGAGCCAGTGGATCTTG
CAPNS1	calpain, small subunit 1	NM_001749	ATGGTTTTGGCATTGACACATG	GCTTGCCTGTGGTGTCGC

[a] Conditions are available upon request

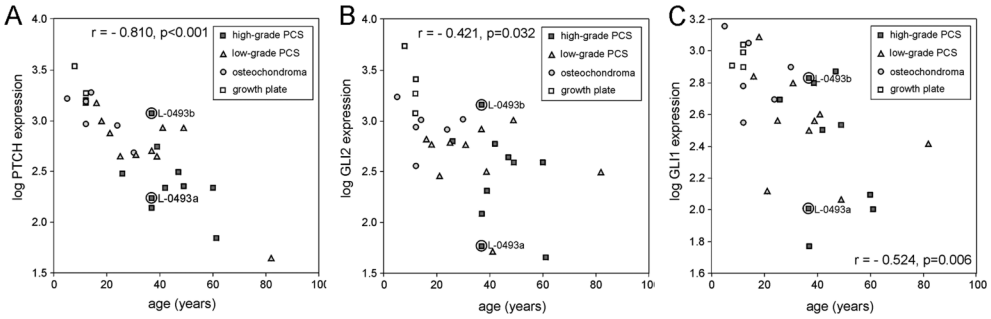

Supplementary figure 5.1. Correlation between expression of IHH signalling and patient's age. Log transformed relative mRNA expression levels in growth plate, osteochondromas, low-grade and high-grade chondrosarcomas of (A) *PTCH*, (B) *GLI2* and (C) *GLI1* expression. The expression is related to the patient's age. The Pearson correlation is given with corresponding p-value. All three genes have a negative correlation with age. The two samples of L-0493 are circled.

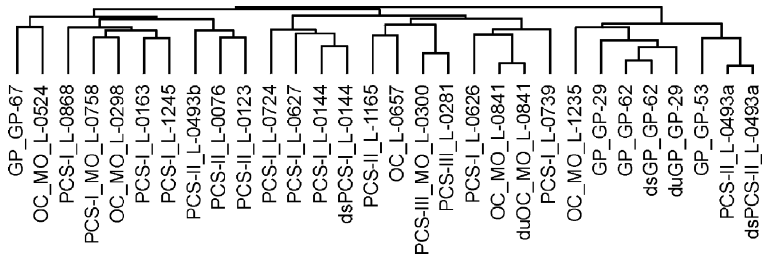

Supplementary figure 5.2. Dendogram of unsupervised cluster analysis. Unsupervised clustering of 3074 gene expression ratios for cDNA that gave interpretable results in at least 70% of the samples. The duplicate (du) and dye swap (ds) cluster together with their original sample.
GP: growth plate; OC: osteochondromas; mo: Multiple Osteochondromas; PCS: peripheral chondrosarcoma.

Supplementary table V.II. Results Limma analysis osteochondroma vs growth plate

Lower expressed in osteochondromas compared to growth plates

Symbol	Accession	Title	p-value	B	log2-fold change GP/OC
SPP1	NM_000582	secreted phosphoprotein 1 (osteopontin)	0.00011	6.6144	4.407
SPP1	AA775616	secreted phosphoprotein 1 (osteopontin)	0.00011	6.9589	3.818
RB1	AA045192	retinoblastoma 1 (including osteosarcoma)	0.00435	2.4186	2.646

Higher expressed in osteochondromas compared to growth plates

Symbol	Accession	Title	p-value	B	log2-fold change GP/OC
KAL1	H17882	Kallmann syndrome 1 sequence	0.00005	8.7842	-3.344
JUNB	T99236	jun B proto-oncogene	0.00009	7.8643	-3.658
JUNB	NM_002229	jun B proto-oncogene	0.00011	7.2865	-3.109
JUNB	N94468	jun B proto-oncogene	0.00011	6.6544	-3.277
	H59614	Homo sapiens, clone MGC:52263 IMAGE:4123447, mRNA, complete cds	0.00011	6.7460	-3.299
JUNB	T99236	jun B proto-oncogene	0.00025	5.7647	-4.221
MT1G	H53340	metallothionein 1G	0.00034	5.3502	-3.081
JUNB	N94468	jun B proto-oncogene	0.00057	4.6656	-2.692
FOSB	T62179	FBJ murine osteosarcoma viral oncogene homolog B	0.00117	3.9810	-4.035
IGFBP5	H08560	insulin-like growth factor binding protein 5	0.00308	2.8145	-2.512
IGF2	N74623	insulin-like growth factor 2 (somatomedin A)	0.00352	2.7383	-2.828
MT1B	H72722	metallothionein 1B (functional)	0.00642	1.9386	-2.112
MT1E	AA872383	metallothionein 1E (functional)	0.00642	1.9411	-3.406
	AA598601	LOC340291	0.01069	1.3640	-2.765

Supplementary table V.III. Genes differentially expressed between grade I and grade III chondrosarcoma

A. Downregulated in peripheral chondrosarcoma grade III compared to peripheral chondrosarcoma grade I
Group comparison method

Symbol[a]	Accession	Title	p-value	FDR[b]	log2-fold change PCSI/PCSIII
COL2A1	N66737	collagen, type II, alpha 1	6.3E-06	0.008	2.682
	AI493835		8.3E-05	0.020	1.670
LAMR1	AA629897	laminin receptor 1 (ribosomal protein SA, 67kDa)	0.0001	0.029	1.218
RPS21	AI681381	ribosomal protein S21	0.0002	0.034	1.855
COX8	AA862813	cytochrome c oxidase subunit VIII	0.0003	0.038	3.080
	AA625788	hypothetical protein IMAGE3455200	0.0005	0.045	2.009
LOC51142	AA454611	16.7Kd protein	0.0005	0.045	1.623
NDUFB8	AI096694	NADH dehydrogenase 1 beta subcomplex, 8, 19kDa	0.0006	0.045	2.070
CDIPT	AA430520	CDP-diacylglycerol--inositol 3-phosphatidyltransferase	0.0006	0.045	1.003
S100B	AA424045	S100 calcium binding protein, beta (neural)	0.0008	0.050	2.504
TUBB2	AA888148	tubulin, beta, 2	0.0008	0.050	1.307
	H72027		0.0009	0.050	1.938
PRCP	AI360366	prolylcarboxypeptidase (angiotensinase C)	0.0009	0.050	1.616
FAH	H44956	fumarylacetoacetate hydrolase (fumarylacetoacetase)	0.0010	0.053	2.120
ILT7	N62837	leukocyte immunoglobulin-like receptor, subfamily A, member 4	0.0010	0.054	1.642
COL9A2	AI493478	collagen, type IX, alpha 2	0.0011	0.060	3.129
PLOD2	H99816	procollagen-lysine, 2-oxoglutarate 5-dioxygenase 2	0.0012	0.061	1.942
UQCR	AA629862	ubiquinol-cytochrome c reductase (6.4kD) subunit	0.0018	0.074	1.147
SERPINH1	R71440	serine (or cysteine) proteinase inhibitor, clade H, member 1	0.0018	0.074	0.943
CTCF	NM_006565	CCCTC-binding factor (zinc finger protein)	0.0021	0.080	0.855
VPS4A	NM_013245	vacuolar protein sorting 4A (yeast)	0.0025	0.095	1.097
C6orf49	AA670330	chromosome 6 open reading frame 49	0.0027	0.097	1.383
CRIP1	AA873604	cysteine-rich protein 1 (intestinal)	0.0027	0.097	1.685

Limma

Symbol	Accession	Title	p-value	B[c]	log2-fold change PCSI/PCSIII
AKR1C3	AA916325	aldo-keto reductase family 1, member C3	0.0056	2.764	2.592
SERPINB2	T49159	serine (or cysteine) proteinase inhibitor, clade B, member 2	0.0095	1.934	3.250
ALDOC	T77281	aldolase C, fructose-bisphosphate	0.0095	1.680	2.429
FGFR3	AA417654	fibroblast growth factor receptor	0.0213	0.423	2.768
TNNT3	AA449932	troponin T3, skeletal, fast	0.0261	0.199	4.818

B. Upregulated in peripheral chondrosarcoma grade III compared to peripheral chondrosarcoma grade I

Group comparison method

Symbol[a]	Accession	Title	p-value	FDR	log2-fold change PCSI/PCSIII
JUP	R06417	junction plakoglobin	1.0E-06	0.002	-2.565
SERPINE2	**N59721**	**serine (or cysteine) proteinase inhibitor, clade E , member 2**	**1.1E-05**	**0.008**	**-2.565**
AA496013	AA496013		1.4E-05	0.008	-1.171
	R16596		1.4E-05	0.008	-1.506
MMP14	N33214	matrix metalloproteinase 14 (membrane-inserted)	3.3E-05	0.012	-2.490

Supplementary table V.III continued

MMP14	N33214	matrix metalloproteinase 14 (membrane-inserted)	3.3E-05	0.012	-2.490
JUN	**W96155**	**v-jun sarcoma virus 17 oncogene homolog (avian)**	**3.3E-05**	**0.012**	**-3.211**
RAC2	AA521232	ras-related C3 botulinum toxin substrate 2	3.8E-05	0.012	-2.786
PYGB	**AA922705**	**phosphorylase, glycogen; brain**	**5.3E-05**	**0.015**	**-3.059**
THBS1	**AA464630**	**thrombospondin 1**	**6.1E-05**	**0.016**	**-2.826**
OS-9	AA013336	amplified in osteosarcoma	0.0001	0.028	-1.462
LAMB1	**AA446251**	**laminin, beta 1**	**0.0002**	**0.033**	**-3.626**
RBBP4	AA429422	retinoblastoma binding protein 4	0.0002	0.033	-1.938
LIF	R50354	leukemia inhibitory factor	0.0002	0.037	-3.252
TGFB1	R36467	transforming growth factor, beta 1	0.0003	0.044	-1.523
KHK	T61308	ketohexokinase (fructokinase)	0.0003	0.044	-1.286
SERPINE2	**N59721**	**serine (or cysteine) proteinase inhibitor, clade E**	**0.0004**	**0.045**	**-2.396**
MGC20576	H50993	hypothetical protein MGC20576	0.0004	0.045	-1.241
LAMA4	**R43734**	**laminin, alpha 4**	**0.0004**	**0.045**	**-1.727**
	T70421	Human HepG2 partial cDNA, clone hmd5d04m5.	0.0005	0.045	-1.269
JUP	R06417	junction plakoglobin	0.0005	0.045	-2.252
SMG1	NM_014006	PI-3-kinase-related kinase SMG-1	0.0005	0.045	-1.272
CDKN1A	**NM_000389**	**cyclin-dependent kinase inhibitor 1A (p21, Cip1)**	**0.0005**	**0.045**	**-2.889**
	T99236		0.0006	0.045	-1.653
BTG1	**N70463**	**B-cell translocation gene 1, anti-proliferative**	**0.0006**	**0.045**	**-2.635**
CDC42EP1	**H73234**	**CDC42 effector protein (Rho GTPase binding) 1**	**0.0006**	**0.045**	**-2.120**
JUN	**W96155**	**v-jun sarcoma virus 17 oncogene homolog (avian)**	**0.0006**	**0.045**	**-2.071**
	T99236		0.0007	0.049	-1.737
FN1	**R62612**	**fibronectin 1**	**0.0007**	**0.050**	**-1.884**
FN1	**R62612**	**fibronectin 1**	**0.0008**	**0.050**	**-1.889**
D2S448	AI356709	Melanoma associated gene	0.0008	0.050	-1.272
CXCL2	R50407	chemokine (C-X-C motif) ligand 2	0.0008	0.050	-2.012
LATS2	N64139	Homo sapiens, clone IMAGE:4816693, mRNA	0.0008	0.050	-2.442
FAT	NM_005245	FAT tumor suppressor homolog 1 (Drosophila)	0.0008	0.050	-1.742
JUNB	NM_002229	jun B proto-oncogene	0.0010	0.052	-1.653
PES1	R13806	pescadillo homolog 1, containing BRCT domain	0.0010	0.056	-3.411
JUNB	NM_002229	jun B proto-oncogene	0.0012	0.061	-1.318
FN1	**R62612**	**fibronectin 1**	**0.0013**	**0.066**	**-1.613**
FYN	N66144	FYN oncogene related to SRC, FGR, YES	0.0014	0.067	-1.966
	T99236		0.0014	0.068	-2.029
KATNB1	NM_005886	katanin p80 (WD40-containing) subunit B 1	0.0014	0.068	-1.117
KIAA1691	N78076	KIAA1691 protein	0.0015	0.068	-0.946
PEG10	H51765	paternally expressed 10	0.0015	0.068	-4.211
FLJ11126	NM_018332	hypothetical protein FLJ11126	0.0016	0.072	-1.336
CDKN1A	**NM_000389**	**cyclin-dependent kinase inhibitor 1A (p21, Cip1)**	**0.0017**	**0.074**	**-3.900**
CDKN1A	**NM_000389**	**cyclin-dependent kinase inhibitor 1A (p21, Cip1)**	**0.0017**	**0.074**	**-3.211**
	H56918	Human clone 23933 mRNA sequence	0.0018	0.074	-2.035
GATA1	R06446	GATA binding protein 1 (globin transcription factor 1)	0.0018	0.074	-2.816
PRKCA	AA030029	protein kinase C, alpha	0.0018	0.074	-1.989
IMP-2	AA634300	IGF-II mRNA-binding protein 2	0.0018	0.074	-3.265
TCF12	H98856	transcription factor 12	0.0020	0.077	-4.381

Supplementary table V.III continued

POFUT1	T91958	protein O-fucosyltransferase 1	0.0025	0.096	-2.279
MUM2	AA416665	MUM2 protein	0.0026	0.097	-1.168
MAPK10	T75436	mitogen-activated protein kinase 10	0.0027	0.097	-0.776
DDX5	H27564	DEAD/H (Asp-Glu-Ala-Asp/His) box polypeptide 5	0.0028	0.100	-3.023
IGF2	**N74623**	**insulin-like growth factor 2 (somatomedin A)**	**0.0031**	**0.100**	**-2.506**
SERPINE1	N75719	serine (or cysteine) proteinase inhibitor, clade E , member 1	0.0032	0.100	-2.322

Limma Symbol[a]	**Accession**	**Title**	**p-value**	**B**	**log2-fold change PCSI/PCSIII**
LAMB1	**AA446251**	**laminin, beta 1**	**0.0012**	**6.418**	**-3.386**
MSCP	T50082	mitochondrial solute carrier protein	0.0013	5.723	-3.324
FN1	**N26285**	**fibronectin 1**	**0.0031**	**4.561**	**-3.607**
CDKN1A	**NM_000389**	**cyclin-dependent kinase inhibitor 1A (p21, Cip1)**	**0.0048**	**3.748**	**-3.449**
BTG1	**N70463**	**B-cell translocation gene 1, anti-proliferative**	**0.0050**	**3.332**	**-3.342**
IGF2	**N74623**	**insulin-like growth factor 2 (somatomedin A)**	**0.0056**	**2.931**	**-3.450**
ATF3	H21041	activating transcription factor 3	0.0056	2.762	-4.101
JUN	**W96155**	**v-jun sarcoma virus 17 oncogene homolog (avian)**	**0.0064**	**2.523**	**-2.692**
LUM	AA453712	lumican	0.0091	2.164	-3.913
FGFR4	AA446994	fibroblast growth factor receptor 4	0.0095	1.789	-2.736
SERPINE2	**N59721**	**serine (or cysteine) proteinase inhibitor, clade E, member 2**	**0.0095**	**1.860**	**-2.742**
TRAP240	AA457462	thyroid hormone receptor-associated protein, 240 kDa subunit	0.0095	1.921	-2.860
LSS	AA434024	lanosterol synthase (2,3-oxidosqualene-lanosterol cyclase)	0.0095	1.704	-3.764
ST13	H65676	suppression of tumorigenicity 13 (Hsp70 interacting protein)	0.0127	1.383	-2.030
PYGB	**AA922705**	**phosphorylase, glycogen; brain**	**0.0136**	**1.237**	**-2.653**
CDKN1A	**NM_000389**	**cyclin-dependent kinase inhibitor 1A (p21, Cip1)**	**0.0136**	**1.204**	**-3.352**
IGF2	N54596	insulin-like growth factor 2 (somatomedin A)	0.0136	1.214	-3.657
MMP16	H09997	matrix metalloproteinase 16 (membrane-inserted)	0.0176	0.806	-2.570
RGS3	AI369623	regulator of G-protein signalling 3	0.0176	0.902	-3.100
CDC42EP1	**H73234**	**CDC42 effector protein (Rho GTPase binding) 1**	**0.0205**	**0.619**	**-2.458**
THBS1	**AA464630**	**thrombospondin 1**	**0.0205**	**0.587**	**-3.580**
PLOD3	AA459305	procollagen-lysine, 2-oxoglutarate 5-dioxygenase 3	0.0213	0.408	-2.495
PCNA	AA450265	proliferating cell nuclear antigen	0.0213	0.437	-3.009
LAMA4	**R43734**	**laminin, alpha 4**	**0.0213**	**0.477**	**-3.229**
BC002942	AA481481	hypothetical protein BC002942	0.0271	0.076	-2.223
SLC39A1	AA453577	solute carrier family 39 (zinc transporter), member 1	0.0271	0.035	-3.030
RPS3	NM_001005	ribosomal protein S3	0.0271	0.069	-3.829

[a] The genes found in both analyses are indicated in bold
[b] FDR: False discovery rate < 0.1 (10%)
[c] B: log-odds that a gene is differentially expressed